

Graphic mathematical modelling of calcium ion binding dependent vesicle exocytosis in the presynaptic terminal of a central synapse

MAGGIE WILBERFORCE

Integrated Science Program, Class of 2021, McMaster University

SUMMARY

A fundamental aspect of neuroscience is understanding the function of the chemical synapse. To relay electrical signals from neuron to neuron, synaptic vesicles fuse with the presynaptic terminal, undergoing exocytosis to release neurotransmitters into the synaptic cleft. Vesicle exocytosis is a stochastic process which relies on the presence, diffusion, and chelation of calcium ions (Ca^{2+}). These ions enter the presynaptic terminal upon depolarization by action potentials. Accordingly, this study used graphic modelling in Python to examine the spatial and temporal interactions of Ca^{2+} , chelators, and synaptic vesicles in the presynaptic terminal to determine the effects of Ca^{2+} binding to vesicle-associated Ca^{2+} binding targets on the release probability of synaptic vesicles. A two-dimensional model of the presynaptic terminal was constructed, employing the Monte Carlo Method to represent the probabilistic nature of Ca^{2+} conductance and vesicle fusion in the terminal. For observable effect, the model was animated and the initial locations of Ca^{2+} and chelators were allowed to vary randomly while controlling the initial conditions of Ca^{2+} , chelator, and vesicle counts. This model found a positive correlation between Ca^{2+} count and vesicle exocytosis, and a negative correlation between buffer count and vesicle exocytosis. This allowed important microscopic trends to be observed in a physiologically accurate macroscopic way.

Received: 03/03/2020

Accepted: 03/24/2020

Published: 11/24/2020

Keywords: synaptic vesicle, chelator, neurotransmission, chemical synapse, graphic modelling, Monte Carlo Method, Brownian motion, exocytosis

INTRODUCTION

SYNAPSES AND NEUROTRANSMISSION

One of the most important mechanisms in the nervous system is neurotransmission, which includes neuron-neuron and neuron-effector communication (Bean, 2007). Without neurotransmission, electrical signals would not propagate between cells, limiting the distance through which neural signals could be received

and interpreted (Tortora and Derrickson, 2017). The process of neurotransmission is observed throughout the nervous system at synapses, where either two neuronal cells, or a neuron and its target meet (Tortora and Derrickson, 2017). There are two types of synapses, electrical and chemical (Hall, 2016).

While electrical synapses are important for synchronous muscle contraction in smooth and cardiac muscle (Tortora and Derrickson, 2017),

the most prevalent type of synapse in the nervous system is the chemical synapse (Nicholls et al., 2012). Chemical synapses arise where plasma membranes of adjacent cells do not come into contact, creating an area called the synaptic cleft (Ma, 2014). Action potentials do not directly propagate across the synaptic cleft and instead must be converted into chemical signals. These chemical signals can then trigger secondary electrical impulses in the receiving cell (Ma, 2014).

CHEMICAL NEUROTRANSMISSION

Chemical neurotransmission (see Figure 1) is the conduction of action potentials between adjacent cells at a chemical synapse (Tortora and Derrickson, 2017). The extracellular and intracellular ion concentrations of the presynaptic terminal play a vital role in the conversion of the electrical stimulus to a chemical signal (Tortora and Derrickson, 2017).

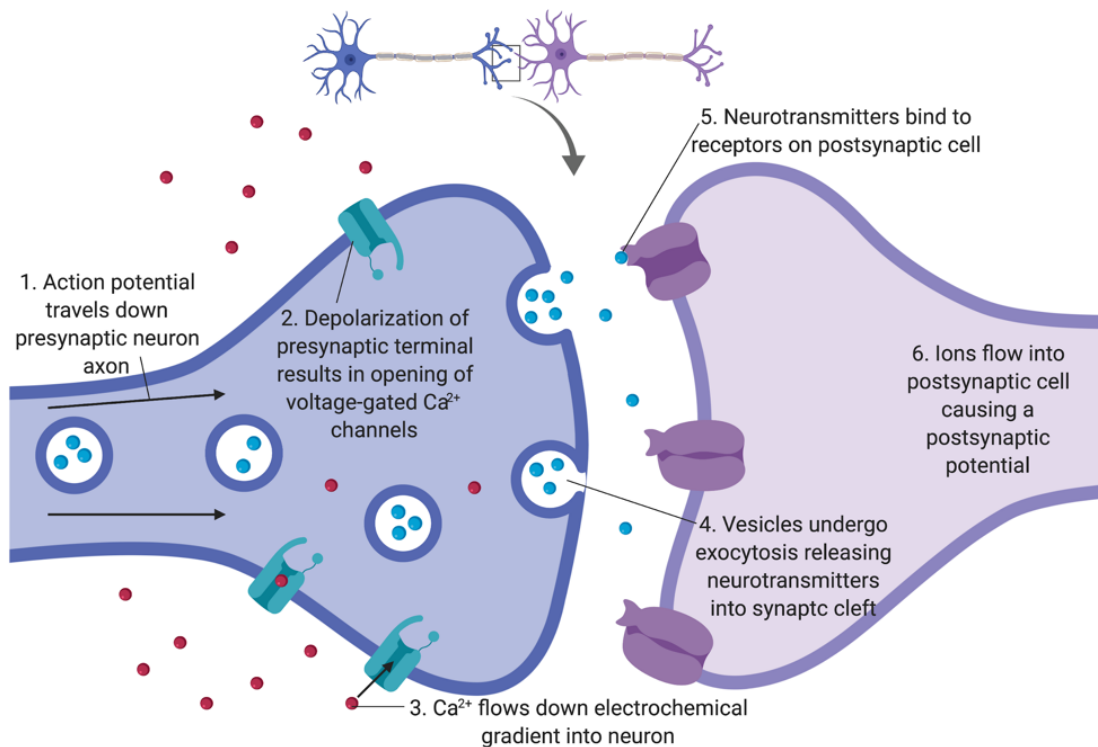


Figure 1: Diagram outlining the process of chemical neurotransmission. Note that the region in blue represents the presynaptic terminal, also known as the synaptic end bulb, while the purple region represents a neighbouring neuron (self-adapted using BioRender.com, 2019).

Electrical signals are converted into a chemical signal via the release of neurotransmitters from the presynaptic membrane following an action potential (Tortora and Derrickson, 2017). The neurotransmitters then diffuse through the interstitial fluid in the synaptic cleft and bind to receptors on the plasma membrane of the postsynaptic cell. Binding to these receptors allows various ion channels to be opened, creating a subsequent potential in the postsynaptic cell (Tortora and Derrickson, 2017).

As an action potential travelling down the axon of a neuron approaches the presynaptic end bulb, it depolarizes the plasma membrane surrounding the terminal (Tortora and Derrickson, 2017). In doing so, it opens voltage-gated calcium ion (Ca^{2+}) channels found along the terminal membrane (Harasym, 2018). Since the Ca^{2+} concentration in the extracellular fluid is higher than that of the intracellular fluid, Ca^{2+} are able to flow down their electrochemical gradient into the synaptic end bulb (Tortora and Derrickson, 2017). Increased

Ca^{2+} concentration within the presynaptic terminal is the signal which initiates exocytosis of synaptic vesicles from an area of the presynaptic terminal membrane called the active zone (Tortora and Derrickson, 2017; Purves et al., 2001). These vesicles merge with the plasma membrane of the presynaptic terminal, releasing the neurotransmitters contained within them into the synaptic cleft (Purves et al., 2001). Once in the cleft, they will diffuse through the interstitial fluid and bind to postsynaptic cell receptors. Binding of these receptors allows ions to flow into the postsynaptic cell, altering the voltage difference across the postsynaptic membrane to create a postsynaptic potential (Tortora and Derrickson, 2017). Despite the depolarizing effect of the excitatory signal from the presynaptic neuron, the response in the postsynaptic cell may be either depolarizing and excitatory or hyperpolarizing and inhibitory - depending on the ions which flow into the postsynaptic terminal. If the sum of postsynaptic potentials eventually reaches threshold, it will trigger an action potential in the postsynaptic cell, leading to further conduction of this neural impulse (Tortora and Derrickson, 2017).

VESICLE EXOCYTOSIS AND THE ROLE OF Ca^{2+}

While the conduction of electrical impulses across chemical synapses is well understood, the more precise mechanisms by which synaptic vesicles undergo exocytosis at the active zone remain a topic of debate within the scientific community (Purves et al., 2001). It is known that a Ca^{2+} influx from the interstitial fluid surrounding the presynaptic terminal is essential to vesicle release (Shahrezaei and Delaney, 2004), but the mechanism used by Ca^{2+} to initiate synaptic vesicle exocytosis requires further exploration (Tyler and Murthy, 2004).

When Ca^{2+} flow into the presynaptic terminal via voltage-gated Ca^{2+} channels, they have the ability to interact with two cellular structures: Ca^{2+} chelators or vesicle-associated Ca^{2+} binding targets on docked synaptic vesicles (Kennedy, Piper and Atwood, 1999). If they interact with Ca^{2+} chelators, their ability to diffuse through the presynaptic terminal is compromised, decreasing their free concentrations as the chelators buffer the Ca^{2+} in the cytoplasm (Kennedy, Piper and

Atwood, 1999). If they are in close enough proximity to synaptic vesicles, however, they can bind to vesicle proteins that mediate the fusion of the vesicular membrane with that of the active zone (Kennedy, Piper and Atwood, 1999; Südhof, 2012). The presence of Ca^{2+} chelators and vesicle-associated Ca^{2+} binding targets is key to the probability with which Ca^{2+} will bind to synaptic vesicles initiating exocytosis. The Ca^{2+} chelators moderate the extent of Ca^{2+} nano- and microdomains surrounding each voltage-gated Ca^{2+} channel, affecting the number of Ca^{2+} that become bound to vesicles (Stanley, 2015). In general, the concentration of Ca^{2+} in the presynaptic terminal is transient, creating a Ca^{2+} microdomain that dissipates as the distance from the Ca^{2+} channel increases. This is partially due to the buffers throughout the presynaptic terminal that are constantly removing Ca^{2+} from the environment (Stanley, 2015). Consequently, for Ca^{2+} -binding dependent synaptic vesicle-associated exocytosis to be successful, voltage-gated Ca^{2+} channels must be found relatively close to the synaptic vesicles themselves (Kennedy, Piper and Atwood, 1999).

The binding of four or five Ca^{2+} to vesicle-associated binding targets initiates various processes that result in exocytosis (Stanley, 2015). While these processes are not well understood, it is widely accepted that they involve soluble N-ethylmaleimide-sensitive factor attachment protein receptors or SNARE proteins (Tyler and Murthy, 2004). It is hypothesized that a SNARE complex, which is composed of syntaxin and synaptosomal nerve-associated protein 25 on the active zone membrane, and synaptobrevin on the vesicular membrane, initiates the creation of a fusion pore between the presynaptic membrane and the vesicle (Ma, 2014). This process is then accelerated, and the pore is enlarged to accommodate exocytosis when Ca^{2+} binds to a receptor known as synaptotagmin on the vesicular membrane, which interacts with the SNARE complex (Tyler and Murthy, 2004; Ma, 2014). This interaction allows exocytosis to be completed, releasing neurotransmitters into the synaptic cleft to diffuse to the postsynaptic membrane (Tyler and Murthy, 2004).

GRAPHIC MATHEMATICAL MODELLING AND THE MONTE CARLO METHOD

Since cellular processes are so difficult to visualize due to the scale and rapid speed of the interactions, mathematical modelling has become a common platform for the examination of cellular mechanisms. Probabilistic situations, such as the modelling of a presynaptic terminal often require a complex analysis, which can be accomplished using a combination of graphic modelling and the Monte Carlo Method (Najarian, 2019).

The Monte Carlo Method is a common technique used in the mathematical simulation of stochastic processes (Lafortune, 1995), as it generates results based on a random distribution of numbers (Gentle, 2010). Although simplified, this method of analysis essentially takes a problem which is typically dependent on a probability distribution and generalizes it to follow a deterministic model in which a set of inputs yields a distinct set of outputs. This model is then iterated using a sample of pseudorandom numbers as inputs at each step based on the designated probability distribution, accounting for the probabilistic nature of the event (Gentle, 2010). The Monte Carlo Method is often used in conjunction with graphic modelling to visualize the processes that occur spatially and temporally in a stochastic mechanism (Kennedy, Piper and Atwood, 1999).

To demonstrate graphic mathematical models of synapses, the Monte Carlo Method allows the micro-movements that occur throughout the conduction of an electrical impulse to be simulated (Kennedy, Piper and Atwood, 1999). Exploring this mechanism using simple deterministic mathematics is challenging since the diffusion of ions, such as Ca^{2+} , throughout the presynaptic terminal is entirely random, while the opening of voltage-gated Ca^{2+} channels and exocytosis of synaptic vesicles follow probability distributions. The Monte Carlo Method, however, allows a model of these processes to be iterated so that while the inputs at each step yield very specific outputs, the outputs of the entire model demonstrate time evolution. This allows the structures under investigation to be monitored for any trends in behaviour. Many iterations can be completed in a short period of time so that long-term synaptic behaviours can be evaluated and

interpreted. The process of iterating the model allows the random physiological events that occur in the synapse to be explored and visualized so that any stochastic variation is observed (Kennedy, Piper and Atwood, 1999).

PURPOSE OF STUDY

In this investigation, graphic mathematical modelling and the Monte Carlo Method were used in an attempt to explore the relationships between Ca^{2+} influx and synaptic vesicle exocytosis in the presynaptic terminal of a central nervous system synapse. To achieve the most physiologically accurate model possible, this study examined the interactions between diffusing Ca^{2+} and Ca^{2+} chelators, as well as between Ca^{2+} and the vesicles themselves. The hope was to explore the number of synaptic vesicles that undergo exocytosis with each influx of Ca^{2+} , as well as how the buffering of Ca^{2+} affects the rate of exocytosis. The initial spatial distributions of Ca^{2+} and Ca^{2+} chelators were changed at each initialization of the model. This allowed for the effects of random distribution of these cellular structures to be examined while controlling the locations of the synaptic vesicles docked at the active zone. Overall, this graphic model allowed the spatial and temporal relationships between Ca^{2+} , their chelators, and synaptic vesicles docked at the active zone of a central synapse to be explored and visualized.

METHODS

PLATFORM FOR STUDY

The generation of this mathematical model was completed using Python 3.0. The shell of the code itself was based upon a Predator-Prey Simulation model created by Ben Katz in 2011. This model was used as a guide for the code created here but was altered significantly to meet the specifications and physiological expectations of the presynaptic terminal at a central synapse.

ASSUMPTIONS

As this model aimed to be as physiologically accurate as possible, various assumptions were essential to create a model simplistic enough for animation and visual representation. The first assumption was that once the Ca^{2+} entered the presynaptic terminal via theoretical voltage-gated Ca^{2+} channels, they are unable to exit the

presynaptic terminal. While this created a more simplistic model in which initialization could occur, once all of the Ca^{2+} had bound to another component, it is not entirely physiologically correct. In a real presynaptic terminal, there would not only be voltage-gated Ca^{2+} channels allowing Ca^{2+} to flow into the presynaptic terminal, but there would also be Ca^{2+} leak channels, which would allow Ca^{2+} to passively flow out of the presynaptic terminal as its concentrations within the terminal rose (Borst and Sakmann, 1998). The amount of Ca^{2+} flowing out of the terminal, however, is so minute (Kennedy, Piper and Atwood, 1999) that it was assumed negligible in this model and the outflow of Ca^{2+} was not considered. Secondly, this model assumed that, once Ca^{2+} bound to either buffers or synaptic vesicles, this binding was irreversible and the Ca^{2+} would remain bound indefinitely. Yet, in reality the Ca^{2+} bound to both of these structures would eventually dissociate according to its dissociation constant. The rates of dissociation, however, are so slow (one Ca^{2+} dissociation every 1000 microseconds) (Kennedy, Piper and Atwood, 1999) that they were deemed negligible since the time-lapse in this model was only 500 microseconds (Katz and Miledi, 1965). It was also assumed that once a synaptic vesicle underwent exocytosis, it was not replaced by an additional vesicle (Purves et al., 2001; Tyler and Murthy, 2004). Again, this assumption was made due to the scale of the model. Such a small amount of time passed in each run of the model that a new vesicle would not have the time to be docked and primed before the run was complete (Purves et al., 2001; Tyler and Murthy, 2004). The final assumption made was that the presynaptic terminal could be represented by a two-dimensional structure, when in reality, it is three-dimensional space (Siksou et al., 2007). This was assumed to maintain the simplicity but should be considered when interpreting data obtained from the model.

GENERATION OF MODEL

To produce the visual representation of what occurs in the presynaptic terminal of a central synapse, Python was used to generate a canvas on which different components of the synapse were placed and stochastically moved to simulate physiological processes via the Monte Carlo Method (see Appendix for code). The model

yielded a two-dimensional top-view of the presynaptic terminal at a central synapse.

The first steps in making the model involved defining certain parameters associated with the presynaptic terminal and designing the terminal itself. It was decided that the model would run for 1000 iterations each time, where each iteration was 0.5 microseconds for a total time-lapse of 500 microseconds, which aligns with a typical synaptic delay (Katz and Miledi, 1965). The shape of this terminal, or more precisely the active zone of the central synapse's presynaptic terminal, was best approximated by a circle which was placed in the centre of the canvas with a diameter of 350 nm, where one pixel was equivalent to one nm (Südhof, 2012). The synaptic terminal was filled with the colour yellow, while its outline, used to represent its plasma membrane, was coloured black.

Following the generation of the presynaptic terminal, three classes of components, namely vesicles, buffers and Ca^{2+} , were defined. Ten synaptic vesicles (Purves et al., 2001; Tyler and Murthy, 2004), represented by orange circles with diameters of 50 nm (Ma, 2014), were placed along the edge of the presynaptic terminal circle just inside its "membrane" at equal distances from one another. Note that these vesicles were always located in the same position each time the model was initialized. The free buffers were represented by black circular objects, while the free Ca^{2+} were green circles, each of which was the size of four pixels, chosen simply so they could be easily observed. The buffers were defined to move 25/28 of a pixel at each iteration and to be localized to the region within the circle of the presynaptic terminal (Kennedy, Piper and Atwood, 1999). Though the speed of the buffers remained constant at each initialization and iteration, the initial distribution of the buffers within the presynaptic terminal was randomly generated each time, as was the changing direction of these components at each iteration. The Ca^{2+} moved 25/12 of a pixel at each iteration, and though their initial distributions were also randomly generated at each initialization, their locations were not confined to the presynaptic terminal (Kennedy, Piper and Atwood, 1999). Ca^{2+} were randomly dispersed throughout the model at initialization and then were able to diffuse through the interstitial fluid in randomly generated directions. If they flowed into

the presynaptic terminal, they then became confined to this space.

After the classes of vesicles, buffers and Ca^{2+} were defined, the interactions between these classes was explored. Interactions between the buffers and Ca^{2+} were coded such that Ca^{2+} contact with a buffer would result in irreversible binding, assuming the buffer had less than four total Ca^{2+} bound already (Kennedy, Piper and Atwood, 1999). This process removed the Ca^{2+} from free diffusion so that it could no longer interact with any other components. When a buffer was bound to a single Ca^{2+} it would turn blue, while binding to two or three Ca^{2+} caused it to turn purple. Once a buffer had four Ca^{2+} bound, it would turn red, indicating it had reached capacity, and would simply diffuse around the presynaptic terminal without the ability to interact with any components (Kennedy, Piper and Atwood, 1999). Note that when Ca^{2+} bound to buffers the Ca^{2+} component would disappear, and its presence was solely represented by the changing colour of the buffer component. Another coded interaction was

Table 1: Chart outlining the paired counts of calcium ions (Ca^{2+}) and buffers used to collect data from the graphic model.

Number of Ca^{2+} ions	Number of Buffers
80	0
80	80
80	290
80	500
290	0
290	80
290	290
290	500
500	0
500	80
500	290
500	500

that which occurs between free Ca^{2+} present in the presynaptic terminal and the synaptic vesicles. When free Ca^{2+} diffused in the presynaptic terminal such that it contacted a synaptic vesicle, it would bind to this synaptic vesicle irreversibly, changing colour to pink. In this way, the Ca^{2+} would again be removed from freely diffusing in the system. Once five Ca^{2+} had bound to a single vesicle, the vesicle would “disappear” turning yellow, indicating that it had undergone exocytosis with the active zone membrane, releasing its theoretical contents of neurotransmitters into the synaptic cleft (Guerrier and Holcman, 2018). Note that in this model, the buffers were able to come into contact with synaptic vesicles without any interaction or interruption in their diffusion and Ca^{2+} repelled one another due to their mutual positive charges.

GATHERING DATA

To examine the validity of this model and observe the trends occurring in the interactions, various runs of the model were completed to generate results. It is known that the number of Ca^{2+} flowing into the presynaptic terminal at each depolarization is within a range of 80 and 500 ions (Guerrier and Holcman, 2018). Likewise, the number of buffers molecules is also typically within this range (Guerrier and Holcman, 2018). To collect results various pairings of buffer and Ca^{2+} counts were established, with five runs of the model executed for each pairing. The pairings used involved the minimum numbers of buffers and Ca^{2+} , the intermediate number of these components, and the maximum number of each component, as outlined in Table 1. Note that trials were also done with zero buffers to act as a control and to observe the effect of Ca^{2+} on vesicle exocytosis without regulation, while the effect of zero Ca^{2+} was not attempted since Ca^{2+} are vital to vesicle exocytosis. The data gathered from these trials included the number of vesicles that underwent exocytosis in each run and the time with which these vesicles underwent exocytosis.

RESULTS

THE GRAPHIC MODEL

The coding of this mathematical model yielded a two-dimensional animation of the active zone of a central synapse (see Figure 2). While data was collected from this model, a key aspect of its

importance was simply the ability to macroscopically visualize what occurs microscopically in the presynaptic terminal before vesicle exocytosis.

NUMERICAL RESULTS

When interpreting the results from the output of this graphic model (see Table 2 in the Appendix), the first trend observed was the relationship between Ca^{2+} count and the number of vesicles undergoing exocytosis at various buffer counts (see Figure 3). The results showed that as the number of Ca^{2+} increased and the number of buffer molecules decreased, the average number of vesicles undergoing exocytosis increased. The trend, however, seemed to plateau such that the number of vesicles increased more rapidly at lower Ca^{2+} counts than at higher Ca^{2+} counts.

The next trend examined was the relationship between the ratio of buffer molecules to Ca^{2+} in the presynaptic terminal and the average number of vesicles undergoing exocytosis (see Figure 4). It was found that as the ratio of buffers to Ca^{2+} increased, the number of vesicles undergoing exocytosis decreased. However, while this trend was consistent for all Ca^{2+} counts, the same ratios

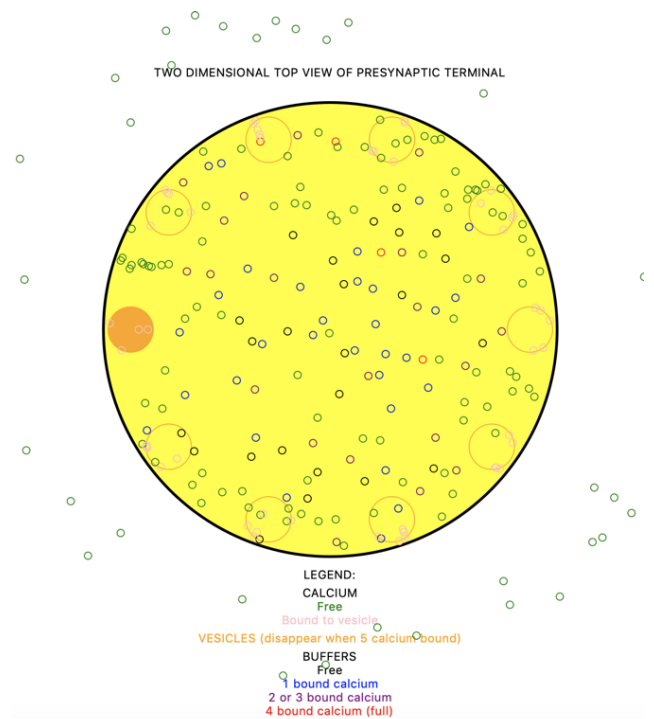


Figure 2: Image capturing a frame of the motion of the generated graphic mathematical model. Note that this run was executed with 80 buffer molecules and 290 Ca^{2+} (self-generated, 2019).

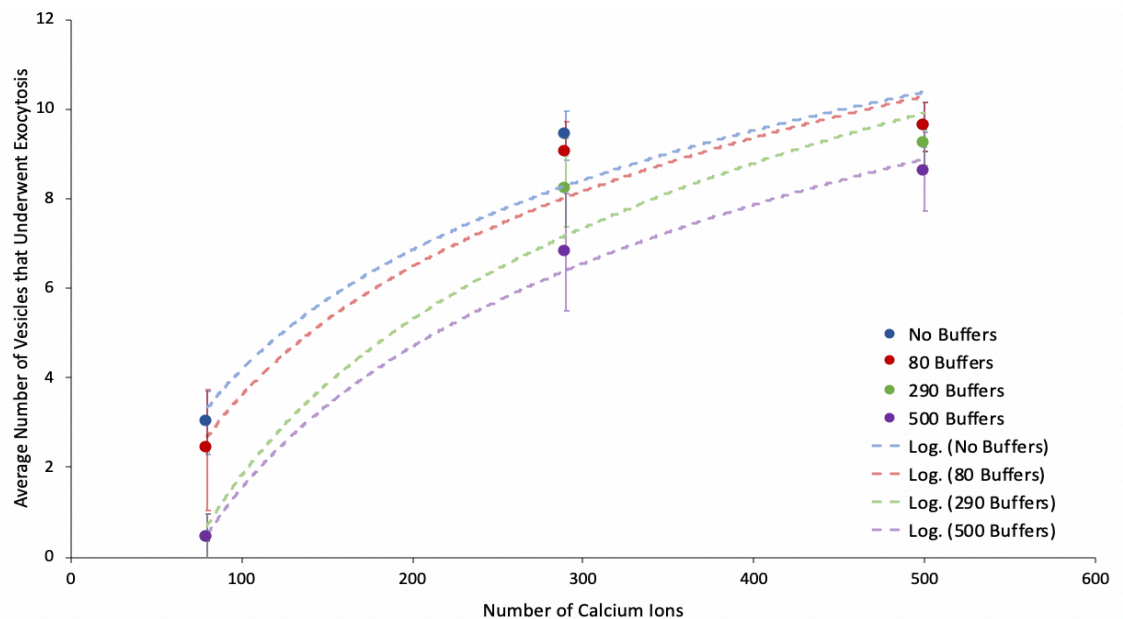


Figure 3: Relationship between calcium ion count and the mean \pm standard deviation number of vesicles that underwent exocytosis in a single run of the graphic model, at various buffer counts. Logarithmic trendlines are also shown with their equations being $y=3.8479\ln(x)-13.530$, $y=4.1443\ln(x)-15.471$, $y=5.0279\ln(x)-21.329$, and $y=4.5637\ln(x)-19.479$ for the no buffers, 80 buffer, 290 buffers and 500 buffers groups, respectively. The R^2 values are 0.9304, 0.9530, 0.9645, and 0.9931, respectively.

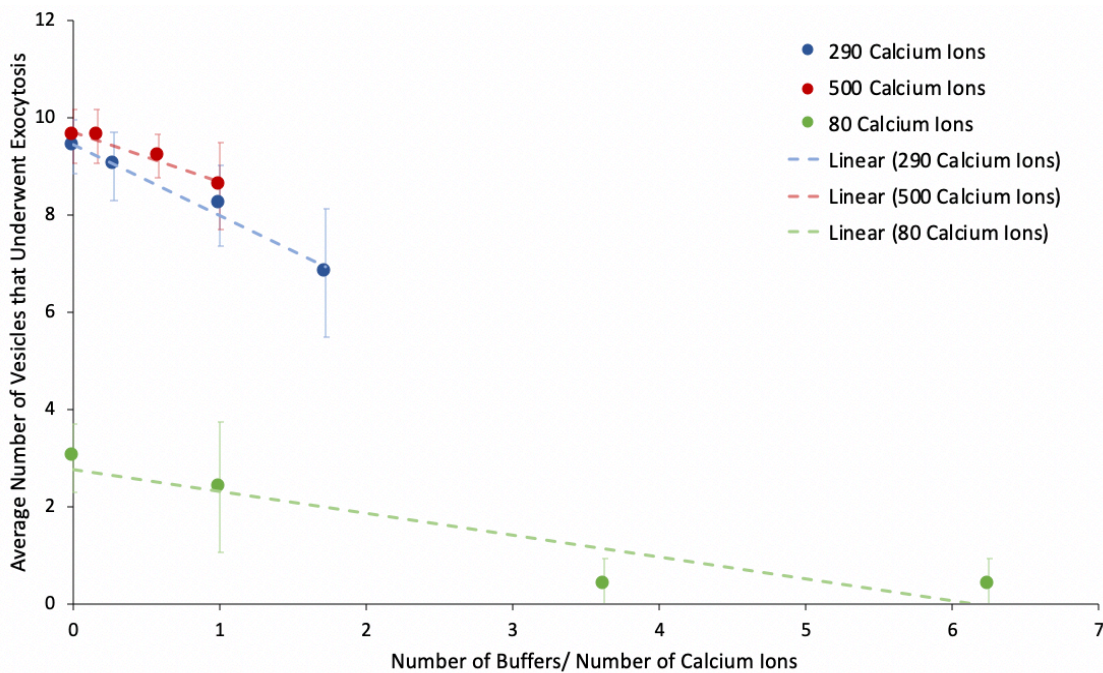


Figure 4: The ratio of buffer molecules to calcium ions (Ca^{2+}) compared to the mean \pm standard deviation number of vesicles undergoing exocytosis. Linear trendlines are also shown with equations of $y = -1.0296x + 9.6979$, $y = -1.4694x + 9.4521$, and $y = -0.4445x + 2.7585$ for the 290 Ca^{2+} , 500 Ca^{2+} , and 80 Ca^{2+} groups, respectively. The R^2 values are 0.9574, 0.9832, and 0.8537, respectively.

of buffer to Ca^{2+} in each of the Ca^{2+} count groups were not identical. Despite having the same relative number of buffers, as Ca^{2+} count increased, the number of vesicles undergoing exocytosis still increased.

Next, the temporal relationships between Ca^{2+} count, buffer count, and vesicle exocytosis were observed. The first relationship was between Ca^{2+} count and the time required for the first vesicle to undergo exocytosis, at varying buffer counts (see Figure 5). It was found that as the number of Ca^{2+} increased and the number of buffer molecules decreased, the time it took for the first vesicular exocytosis decreased. Note, again, that this trend seemed asymptotic, decreasing by less and less as Ca^{2+} count increased. The only exception to the observed trend was that at the 80 Ca^{2+} count, the presence of 500 buffers yielded a lower average time for the first vesicle to undergo exocytosis than the presence of 290 buffer molecules.

The final relationship examined was that between the number of Ca^{2+} , the number of buffer molecules, and the range of time over which vesicular exocytosis occurred (see Figure 6). It was found that as the amount of Ca^{2+} present in the

presynaptic terminal increased, the range of time over which exocytosis occurred also increased. Note that no trend in the relationship between buffer counts and this range of time was observed.

DISCUSSION

THE GRAPHIC MATHEMATICAL MODEL

A key aspect of this model's production was the ability to visualize processes occurring in the presynaptic terminal. In creating this two-dimensional animation, it allows viewers to gain a better understanding of the interactions that occur between components in the terminal.

An important visual aspect of this model was the presence of Brownian motion, or the stochastic movement of particles due to random motion and collisions (Kac, 1947; Kočović, 2011; Metcalfe et al., 2012). Brownian motion, or the random walk theory, is often a difficult concept to understand and visualize. Thus, the small, randomly vibrating components in this model allow this entirely microscopic and abstract idea to be viewed on a

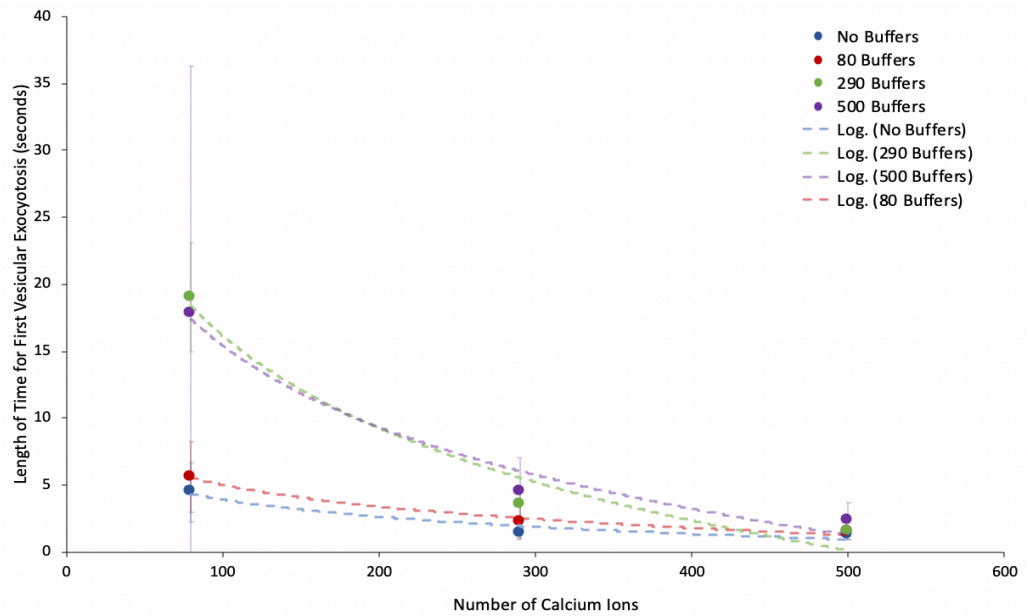


Figure 5: Relationship between the number of calcium ions and the mean \pm standard deviation time required for the first vesicle to undergo exocytosis, at various buffer molecule counts. Logarithmic trendlines are also shown with equations of $y=-1.847\ln(x)+12.413$, $y=-2.319\ln(x)+15.682$, $y=-9.969\ln(x)+62.058$, and $y=-8.793\ln(x)+55.9$ for the no buffers, 80 buffers, 290 buffers, and 500 buffers groups, respectively. The R^2 values are 0.9275, 0.9829, 0.9662, and 0.9748, respectively.

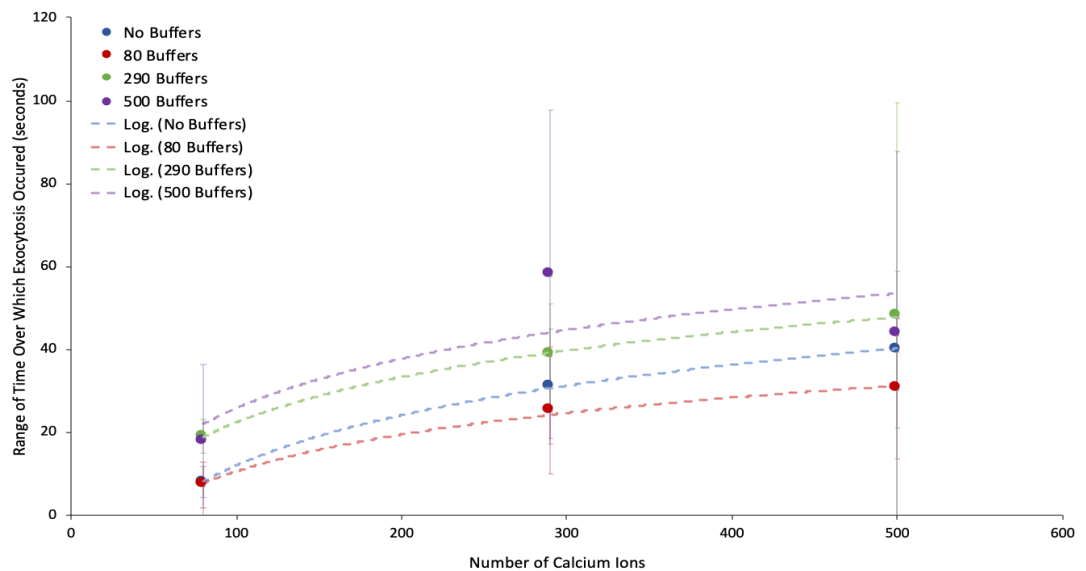


Figure 6: Relationship between the amount of calcium ions and the mean \pm standard deviation range of time over which vesicles underwent exocytosis at various buffer counts. Logarithmic trendlines are also shown with equations of $y=17.506\ln(x)-68.637$, $y=12.861\ln(x)-48.710$, $y=15.800\ln(x)-50.421$, and $y=17.191\ln(x)-53.375$ for the no buffers, 80 buffers, 290 buffers, and 500 buffers groups, respectively. The R^2 values are 0.9995, 0.9943, 0.9991, and 0.6303, respectively.

large scale (Kac, 1947). Brownian motion governs the movement of most microscopic components in fluids and gas, making it vital to the understanding of not only the stochastic function of neurotransmission at chemical synapses, but also for many other biological processes (Kac, 1947; Kočović, 2011).

The presence of this random walk Brownian motion also clarifies the use of the Monte Carlo Method in the creation of this model. Brownian motion, being entirely random (Kac, 1947), cannot be accurately represented using analytical formulas, making it very difficult to interpret and express mathematically. Consequently, the Monte Carlo Method can be applied to virtually simulate the stochastic processes involved in this Brownian motion (Kočović, 2011). Without being able to apply the pseudo-random distribution to the motion of components in this model, as done by the Monte Carlo Method (Kočović, 2011), it would have been impossible to create accurately moving components that mirror the Brownian motion occurring in these physiological processes.

NUMERICAL RESULTS

While examining the relationship between the amount of Ca^{2+} present and the number of vesicles that underwent exocytosis, at various buffer counts, it was not surprising to find an increasing trend. Since vesicle exocytosis is directly controlled by Ca^{2+} binding to vesicle-associated Ca^{2+} binding targets on docked synaptic vesicles (Guerrier and Holcman, 2018; Baumgart et al., 2015), it follows that as the number of Ca^{2+} in the presynaptic terminal rose, so did the number of vesicles that underwent exocytosis (Baumgart et al., 2015). The increased levels of Ca^{2+} in the terminal increased the probability that any one of them might bind to the vesicle-associated target, initiating exocytosis and increasing the number of vesicles that had the opportunity to fuse with the active zone membrane (Catterall, Leal and Nanou, 2013). This same logic supports the fact that, as buffer counts decreased, vesicle exocytosis increased. The decrease in buffering allowed for a greater intracellular presence of free Ca^{2+} , again increasing the probability that Ca^{2+} might bind to a synaptic vesicle receptor (Baumgart et al., 2015). Interestingly, subsequent increases in Ca^{2+} counts resulted in diminishing increases in vesicle exocytosis. One reason for this may have been the

presence of Ca^{2+} - Ca^{2+} repulsion interactions, which occurred due to their mutual positive charges (Kärger, Grinberg and Heitjans, 2005). As the amount of Ca^{2+} increased, the number of repulsive interactions that each ion experienced also increased due to the proximity between the ions. Accordingly, once the amount of Ca^{2+} in the terminal became too abundant, their random diffusion was likely inhibited by the constant repulsive interactions that they experienced, hindering their ability to diffuse freely in the cytoplasm and bind to vesicle receptors (Kärger, Grinberg and Heitjans, 2005). Thus, though an increase in Ca^{2+} increased the probability that Ca^{2+} might bind to a receptor, over time this trend increased diminishingly due to the inhibition of free diffusion caused by Ca^{2+} - Ca^{2+} repulsion. While logical, these repulsion interactions are not something previously described in the literature, and therefore require further study to confirm their presence, as the repulsive interactions may have been amplified in assuming the model to be two-dimensional rather than three-dimensional.

The second relationship explored in this study, between buffer to Ca^{2+} ratio and vesicle exocytosis, demonstrated an inverse trend. This was anticipated because as the number of buffer molecules relative to the amount of Ca^{2+} increased, less free Ca^{2+} was present in the presynaptic terminal, thus decreasing the probability for Ca^{2+} to bind to a vesicle receptor (Baumgart et al., 2015). Though the buffer to Ca^{2+} ratios overlapped between Ca^{2+} count groups, the same ratios in each group did not yield the same number of vesicles undergoing exocytosis. Consequently, Ca^{2+} presence must have a more significant influence on vesicle exocytosis than buffer presence, as the number of vesicles undergoing exocytosis increased with increasing Ca^{2+} count, despite having the same buffer to Ca^{2+} ratio as other groups. This particular trend was not anticipated as it was expected that with the same relative amount of buffering regulating free Ca^{2+} numbers, the same amount of vesicle exocytosis would be observed.

The impact of Ca^{2+} - Ca^{2+} repulsion interactions was again demonstrated with the relationship between the amount of Ca^{2+} and the length of time taken for the first vesicle to undergo exocytosis at various buffer counts. This relationship showed an overall negative trend, which can be explained by

the increased number of Ca^{2+} in the presynaptic terminal. As Ca^{2+} count increased and buffer count decreased, the amount of free Ca^{2+} present in the presynaptic terminal increased, again increasing the probability that Ca^{2+} might bind to a vesicle-receptor (Baumgart et al., 2015). This increased probability can explain how an increased number of Ca^{2+} and decreased buffer counts may decrease the time required for the first vesicular exocytosis. The fact that this trend decreased diminishingly over time, however, can be explained by the possible Ca^{2+} - Ca^{2+} repulsion interactions. When the amount of Ca^{2+} in the presynaptic terminal becomes too abundant, their repulsion interactions will inhibit their ability to freely diffuse throughout the terminal, causing a slight relative decrease in their likelihood of binding vesicle receptors (Kärger, Grinberg and Heitjans, 2005).

The final trend explored in this study was that between the amount of Ca^{2+} at various buffer counts and the range of times over which vesicle exocytosis occurred. The positive relationship observed can be supported by the idea that having more Ca^{2+} present in the presynaptic terminal relative to the number of vesicles in the terminal which remained constant, allowed for the Ca^{2+} count to remain higher for a longer period of time. Accordingly, the probability of Ca^{2+} binding to a vesicle receptor would remain higher longer, thus allowing vesicular exocytosis to occur more readily over this whole time period (Baumgart et al., 2015).

CONCLUSION

One of the most important systems to biological life is the nervous system, which cannot function without neurotransmission. While the general processes behind neurotransmission - specifically at chemical synapses - are relatively well understood, the underlying intricacies of the interactions required for their function are not well explored. In creating this two-dimensional animation of the active zone of the presynaptic terminal of a central synapse, these important

interactions between Ca^{2+} , Ca^{2+} chelators, and synaptic vesicles were visualized in a simplistic manner. In addition, this allowed for a greater understanding of Brownian motion and the applications of the Monte Carlo Method. Examination of the collected data from this model established several important interactions, in particular that increased Ca^{2+} count and decreased buffer counts lead to increased vesicle exocytosis and decreased time for the initial vesicular exocytosis. Other trends identified included that Ca^{2+} - Ca^{2+} repulsion interactions may affect vesicle exocytosis by inhibiting normal Ca^{2+} diffusion and that Ca^{2+} counts play a larger role in the regulation of vesicle exocytosis than buffer counts. While this model requires further exploration to determine its limitations, uncover additional trends, and further examine those already found, it serves as an important first step in visualizing the spatial and temporal interactions occurring in the presynaptic terminal of a central synapse.

ACKNOWLEDGMENTS

First, I would like to thank my supervisor, Dr. George Dragomir, for his support, guidance, and assistance throughout the creation of this model. Without his continued help, the production of this mathematical model would not have been possible. I would also like to thank Dr. Chad Harvey, the Integrated Science Program, and the School of Interdisciplinary Science at McMaster University for facilitating this project.

REFERENCES

- Baumgart, J.P., Zhou, Z.-Y., Hara, M., Cook, D.C., Hoppa, M.B., Ryan, T.A. and Hemmings, H.C., 2015. Isoflurane inhibits synaptic vesicle exocytosis through reduced Ca²⁺ influx, not Ca²⁺-exocytosis coupling. *Proceedings of the National Academy of Sciences*, [online] 112(38), pp.11959–11964. <https://www.doi.org/10.1073/pnas.1500525112>.
- Bean, A., 2007. Chapter 6 - Neuronal Exocytosis. In: *Protein Trafficking in Neurons*. [online] Houston, Texas: Academic Press. pp.97–124. <https://doi.org/10.1016/B978-0-12-369437-9.X5000-2>.
- Borst, J.G.G. and Sakmann, B., 1998. Calcium current during a single action potential in a large presynaptic terminal of the rat brainstem. *The Journal of Physiology*, [online] 506(Pt 1), pp.143–157. <https://www.doi.org/10.1111/j.1469-7793.1998.143bx.x>.
- Catterall, W.A., Leal, K. and Nanou, E., 2013. Calcium Channels and Short-term Synaptic Plasticity. *Journal of Biological Chemistry*, [online] 288(15), pp.10742–10749. <https://www.doi.org/10.1074/jbc.R112.411645/>.
- Gentle, J.E., 2010. Computational Statistics. In: P. Peterson, E. Baker and B. McGaw, eds. *International Encyclopedia of Education (Third Edition)*. [online] Oxford: Elsevier. pp.93–97. <https://www.doi.org/10.1016/B978-0-08-044894-7.01316-6>.
- Guerrier, C. and Holcman, D., 2018. The First 100 nm Inside the Pre-synaptic Terminal Where Calcium Diffusion Triggers Vesicular Release. *Frontiers in Synaptic Neuroscience*, [online] 10(23). <https://www.doi.org/10.3389/fnsyn.2018.00023>.
- Hall, J., 2016. Organization of the Nervous System, Basic Functions of Synapses, and Neurotransmitters. In: *Guyton and Hall Textbook of Medical Physiology*, 13th Edition. [online] United States of America: Elsevier. pp.577–593.
- Harasym, D., 2018. *The Effect of Long-Term Exercise on Neurotransmission*. [online] McMaster University.
- Kac, M., 1947. Random Walk and the Theory of Brownian Motion. *The American Mathematical Monthly*, [online] 54(7), pp.369–391. Available at: <https://www.jstor.org/stable/2304386> [Accessed 3 Mar. 2020].
- Kärger, J., Grinberg, F. and Heitjans, 2005. *Diffusion Fundamentals*. Berlin: Leipziger Universitätsverlag.
- Katz, B., 2011. BuildIts: Predator-Prey Simulation. [Blogspot] Build Its. Available at: <http://build-its.blogspot.com/2011/08/predator-prey-simulation.html> [Accessed 3 Mar. 2020].
- Katz, B. and Miledi, R., 1965. The measurement of synaptic delay, and the time course of acetylcholine release at the neuromuscular junction. *Proceedings of the Royal Society of London. Series B. Biological Sciences*, [online] 161(985), pp.483–495. <https://www.doi.org/10.1098/rspb.1965.0016>.
- Kennedy, K., Piper, S. and Atwood, H., 1999. Synaptic vesicle recruitment for release explored by Monte Carlo simulation at the crayfish neuromuscular junction. *Canadian Journal of Physiology and Pharmacology*, [online] 77(9), pp.634–650. <https://www.doi.org/10.1139/y99-071>.
- Kočović, P., 2011. Brownian motion development for monte carlo method applied on european style option price forecasting. *International Journal of Economics & Law*, 1(1), pp.1–170.
- Lafortune, E., 1995. *Mathematical Models and Monte Carlo Algorithms for Physically Based Rendering*. [online] Flemish Institute for the Promotion of Scientific and Technological Research in the Industry.
- Ma, J., 2014. *Quantitative simulation of synaptic vesicle release at the neuromuscular junction*. [online] Carnegie Mellon University.
- Metcalfe, G., Speetjens, M.F.M., Lester, D.R. and Clercx, H.J.H., 2012. Beyond Passive: Chaotic Transport in Stirred Fluids. In: E. van der Giessen and H. Aref, eds. *Advances in Applied Mechanics*. [online] Elsevier. pp.109–188. <https://www.doi.org/10.1016/B978-0-12-380876-9.00004-5>.
- Najarian, J.P., 2019. Monte Carlo Techniques. In: *Salem Press Encyclopedia of Science*. [online] Salem Press.
- Nicholls, J., Martin, A., Fuchs, P., Brown, D., Diamond, M. and Weisblat, D., 2012. Chapter 1 - Principles of Signaling and Organization. In: *From Neuron to Brain*, 5th ed. Sunderland, Massachusetts, USA: Sinauer Associates, Inc. pp.3–22.
- Purves, D., Augustine, G.J., Fitzpatrick, D., Katz, L.C., LaMantia, A.-S., McNamara, J.O. and Williams, S.M., 2001. Chapter 5: Synaptic Transmission. In: *Neuroscience*, 2nd ed. [online] Sinauer Associates.
- Shahrezaei, V. and Delaney, K.R., 2004. Consequences of Molecular-Level Ca²⁺ Channel and Synaptic Vesicle Colocalization for the Ca²⁺ Microdomain and Neurotransmitter Exocytosis: A Monte Carlo Study. *Biophysical Journal*, [online] 87(4), pp.2352–2364. <https://www.doi.org/10.1529/biophysj.104.043380>.
- Siksou, L., Rostaing, P., Lechaire, J.-P., Boudier, T., Ohtsuka, T., Fejtová, A., Kao, H.-T., Greengard, P., Gundelfinger, E.D., Triller, A. and Marty, S., 2007. Three-Dimensional Architecture of Presynaptic Terminal Cytomatrix. *The Journal of Neuroscience*, [online] 27(26), pp.6868–6877. <https://www.doi.org/10.1523/JNEUROSCI.1773-07.2007>.
- Stanley, E., 2015. Single calcium channel domain gating of synaptic vesicle fusion at fast synapses; analysis by graphic modeling. *Channels*, [online] 9(5), pp.324–333. <https://www.doi.org/10.1080/19336950.2015.1098793>.
- Südhof, T.C., 2012. The Presynaptic Active Zone. *Neuron*, [online] 75(1), pp.11–25. <https://www.doi.org/10.1016/j.neuron.2012.06.012>.
- Tortora, G. and Derrickson, B., 2017. *Principles of Anatomy & Physiology*. 15th ed. United States of America: John Wiley & Sons, Inc.
- Tyler, W. and Murthy, V., 2004. Synaptic vesicles. *Current Biology*, [online] 14(8), pp.R294–R297. <https://doi.org/10.1016/j.cub.2004.03.046>.

Appendix

Table 2: Chart listing all of the raw microdata collected from the graphic model in this study, including the starting buffer and calcium ion (Ca^{2+}) counts, the total number of vesicles that underwent exocytosis and the times at which these vesicular exocytosis events occurred.

Number of Buffers	Number of Ca^{2+} ions	# of Vesicles that Undergo Exocytosis	Time(s) of Vesicular Exocytosis (seconds)
0	80	3	7.23, 11.29, 11.44
0	80	2	3.22, 13.79
0	80	4	2.66, 4.08, 11.64, 15.68
0	80	3	6.53, 11.58, 11.82
0	80	3	2.76, 2.94, 9.45
80	80	3	4.35, 5.73, 9.39
80	80	3	9.36, 10.44, 12.15
80	80	3	3.39, 10.53, 18.76
80	80	0	N/A
80	80	3	5.36, 10.12, 11.51
290	80	1	16.08
290	80	0	N/A
290	80	0	N/A
290	80	1	21.85
290	80	0	N/A
500	80	1	4.75
500	80	0	N/A
500	80	1	30.88
500	80	0	N/A
500	80	0	N/A
0	290	10	1.8, 2.26, 2.46, 2.91, 3.81, 6.76, 9.33, 13.02, 15.46, 33.34
0	290	9	1.7, 2.23, 2.52, 2.77, 6.13, 8.97, 12.47, 13.45, 17.08
0	290	10	0.88, 2.34, 2.6, 2.81, 3.84, 4.09, 5.39, 15.82, 15.98, 53.97
0	290	9	1.52, 2.16, 2.31, 2.6, 2.79, 3.02, 17.48, 29.29, 30.28
0	290	9	1.06, 1.82, 2.41, 2.67, 3, 6.87, 9.12, 12.18, 27.37
80	290	9	2.89, 3.35, 3.71, 4, 4.36, 5.84, 7.99, 31.3, 51.56

Number of Buffers	Number of Ca ²⁺ ions	# of Vesicles that Undergo Exocytosis	Time(s) of Vesicular Exocytosis (seconds)
80	290	9	1.66, 2.38, 3.55, 3.73, 4.47, 4.72, 8.19, 10.06, 27.05
80	290	9	1.01, 2.05, 2.27, 2.58, 2.96, 3.39, 3.9, 7.03, 7.36
80	290	10	1.42, 1.72, 2.05, 3.48, 4.16, 6.46, 8.49, 17.42, 22.12, 26.76
80	290	8	4.06, 4.99, 5.55, 7.22, 12.03, 15.77, 16.65, 24.52
290	290	8	3.39, 5.03, 5.69, 7.35, 7.75, 24.17, 32.06, 57.66
290	290	7	4.65, 5.44, 5.85, 11.78, 12.61, 19.57, 26.6
290	290	9	2.5, 2.66, 2.81, 4.95, 5.54, 8.37, 11.42, 12.33, 45.24
290	290	8	4.46, 4.95, 5.37, 7.37, 8.21, 20.29, 25.12, 47.51
290	290	9	2.85, 3.01, 3.7, 3.85, 4.91, 9.06, 21.05, 23.79, 34.09
500	290	6	2.08, 6.96, 9.82, 12.88, 14.41, 65.93
500	290	8	5.75, 6.94, 8.36, 9.7, 10.63, 13.02, 17.65, 120.68
500	290	8	4.35, 4.98, 5.64, 6.62, 7.88, 11.64, 22.32, 47.93
500	290	5	8.02, 8.51, 11.1, 12.69, 13.35
500	290	7	2.56, 4.91, 5.16, 5.47, 12.99, 21.13, 64.99
0	500	10	1.2, 2.7, 3.16, 3.42, 3.72, 4.02, 4.33, 4.77, 17.62, 32.63
0	500	9	0.79, 1.92, 3.78, 4.32, 4.54, 5.03, 9.07, 12.19, 62.93
0	500	9	1.55, 1.72, 1.91, 2.11, 2.36, 4.39, 6.39, 8.35, 59.7
0	500	10	1.22, 2.56, 3.08, 3.29, 3.55, 3.87, 5.71, 6.56, 7.16, 21.91
0	500	10	1.82, 3.12, 3.35, 3.64, 3.94, 5.31, 5.86, 8.59, 13.33, 28.79
80	500	9	1.66, 1.82, 1.98, 2.97, 3.36, 3.96, 4.68, 5.08, 5.43
80	500	10	1.9, 2.76, 3.01, 3.28, 4.99, 5.47, 5.83, 12.02, 22.52, 32.6
80	500	10	1.1, 2.58, 2.84, 3.6, 4.34, 4.97, 6.56, 7.83, 8.19, 28.82
80	500	10	1.72, 2.39, 3.45, 3.83, 4.26, 4.8, 5.23, 7.29, 7.92, 44.67
80	500	9	1.1, 1.36, 1.58, 3.84, 4.12, 4.43, 4.89, 5.9, 49.01
290	500	9	1.39, 1.69, 2.01, 3.91, 5.17, 5.44, 6.34, 35.59, 56.3
290	500	9	1.63, 2.71, 3.04, 3.41, 6.07, 7.3, 7.6, 9.23, 20.98
290	500	9	1.76, 2.39, 3.14, 5.21, 5.36, 9.87, 10.35, 12.31, 21.1

Number of Buffers	Number of Ca ²⁺ ions	# of Vesicles that Undergo Exocytosis	Time(s) of Vesicular Exocytosis (seconds)
290	500	9	1.52, 1.86, 2.3, 2.78, 4.15, 8.14, 8.31, 8.57, 13.53
290	500	10	1.19, 2.68, 3.02, 4.35, 6.36, 6.97, 8.66, 12.25, 30.23, 136.25
500	500	9	2.23, 3.88, 6.52, 7.94, 10.04, 11.34, 12.1, 14.96, 20.93
500	500	9	1.46, 2.74, 6.34, 7.21, 12.09, 13.92, 15.48, 15.65, 21.65
500	500	9	1.32, 4.76, 7.59, 8.03, 8.33, 9.02, 12.36, 19.49, 121.12
500	500	7	1.8, 3.75, 6.02, 7.47, 7.98, 9.28, 18.36
500	500	9	4.73, 5.86, 6.22, 6.55, 8.85, 9.41, 14.19, 19.06, 47.83

Full Python 3.0 Code for Mathematical Model

```

import tkinter as tk
from tkinter import *
from sys import getfilesystemencoding
import time
import random
import math
from math import *
import numpy as np
### Global parameters: (values cited in write up)
height = 1000 # made larger to make room for legend
width = 700
x_0 = 100 # top left corner x_coordinate = y_coordinate
x_1 = width - x_0 # bottom right corner x_coordinate = y_coordinate
r_0 = (x_1-x_0)/2 # center of pre-synaptic terminal (disk)
vsize = 25 # vesicle size
vesicle_initial = 10 # initial number of vesicles
buffer_initial = 80 # initial number of buffers
calcium_initial = 290 #initial number of calcium - see below for distribution
runs=1000 # total time (updates)
calcium_release = runs # time steps (updates) until calcium is detached from buffer
psize = 4 # buffer and calcium size
x = psize * 2
maxVattached = 5 # max number of Ca attached to vesicle at one time (changed to 5 from
reading new sources)
maxBattached = 4 # max number of Ca attached to buffer at one time
buffer_speed = 25/18 # buffer speed
calcium_speed = 25/12 # calcium speed
canvas = Canvas(highlightthickness=0, height=height, width=width)
canvas.master.title("Presynaptic Terminal")

```

```

if getfilesystemencoding() == 'utf-8':
    canvas.pack()
### Title
canvas.create_oval(x_0,x_0,x_1,x_1,outline="black", fill="yellow", width=3)
canvas.create_text((x_0+x_1)/2,2*x_0/3,justify='center',text="TWO DIMENSIONAL TOP
VIEW OF PRESYNAPTIC TERMINAL")
### Legend
canvas.create_text((x_0+x_1)/2,x_1+20,justify='center',text="LEGEND:")
canvas.create_text((x_0+x_1)/2,x_1+40,justify='center',text='CALCIUM')
canvas.create_text((x_0+x_1)/2,x_1+55,justify='center',fill='green', text='Free')
canvas.create_text((x_0+x_1)/2,x_1+70,justify='center',fill='pink',text='Bound to vesicle')
canvas.create_text((x_0+x_1)/2,x_1+90,justify='center',fill='orange',text='VESICLES (disappear
when 5 calcium bound)')
canvas.create_text((x_0+x_1)/2,x_1+110,justify='center',text='BUFFERS')
canvas.create_text((x_0+x_1)/2,x_1+125,justify='center',text='Free')
canvas.create_text((x_0+x_1)/2,x_1+140,justify='center',fill='blue',text='1 bound calcium')
canvas.create_text((x_0+x_1)/2,x_1+155,justify='center',fill='purple',text='2 or 3 bound calcium')
canvas.create_text((x_0+x_1)/2,x_1+170,justify='center',fill='red',text='4 bound calcium (full)')
def _create_circle(self, x, y, r, **kwargs):
    return self.create_oval(x-r, y-r, x+r, y+r, **kwargs)
tk.Canvas.create_circle = _create_circle
def _create_circle_arc(self, x, y, r, **kwargs):
    if "start" in kwargs and "end" in kwargs:
        kwargs["extent"] = kwargs["end"] - kwargs["start"]
        del kwargs["end"]
    return self.create_arc(x-r, y-r, x+r, y+r, **kwargs)
tk.Canvas.create_circle_arc = _create_circle_arc
##Converting polar coordinate to cartesian:
def pol2cart_x(theta,r):
    x=(r*math.cos(theta))
    return x
def pol2cart_y(theta,r):
    y=(r*math.sin(theta))
    return y
def component_loc(theta,r,size,color):
    """Defining the locations of the components in the synapse. theta in radians"""
    location =
canvas.create_circle(pol2cart_x(theta,r)+x_0+r_0,pol2cart_y(theta,r)+x_0+r_0,size,outline=color)
    return location
def vesicle_loc(theta,r,size,color):
    """Defining the locations of the components in the synapse. theta in radians"""
    location =
canvas.create_circle(pol2cart_x(theta,r)+x_0+r_0,pol2cart_y(theta,r)+x_0+r_0,size,outline='orange'
,fill=color)
    return location
componentList = []
##### VESICLES #####
class vesicle():

```



```

def __init__(self, attached = 0, status = 'Free', vesicle_initial = vesicle_initial, sector = 0, r_0 =
r_0, vsize = vsize):
    self.type = 'Vesicle'
    self.count = 1
    self.attached = attached
    self.status = status
    self.initial = vesicle_initial
    self.size = vsize
    self.sector = sector
    self.angle = sector*2*pi/self.initial
    self.r_0 = r_0
    self.rad = self.r_0-self.size-5
    if self.attached == maxVattached:
        self.status = 'Full'
    if self.status == 'Free':
        self.color = 'orange'
    else:
        self.color = 'yellow'
        self.count = 0
    self.shape = vesicle_loc(self.angle,self.rad,self.size,self.color)
    self.x = pol2cart_x(self.angle,self.rad)
    self.y = pol2cart_y(self.angle,self.rad)
    self.coords = [self.x, self.y]
    componentList.append(self)
def move(self):
    if self.status == 'Free':
        for component in componentList:
            if ((component.type == 'Calcium') and (component.status == 'Free')):
                distance = math.hypot(self.x-component.x,self.y-component.y)
                if distance < self.size:
                    self.attached += 1
                    component.status = 'V_Bound'
                    component.color = 'pink'
                    component.count = 0
                if self.attached == maxVattached:
                    self.status = 'Full'
                    self.color = 'yellow'
                    self.count = 0
            canvas.delete(self.shape)
            self.shape = vesicle_loc(self.angle,self.rad,self.size,self.color)
def destroy(self):
    return False
##### BUFFERS #####
class Buffer():
    def __init__(self, direction = 0, attached =0, speed = buffer_speed, angle = 0, rad = 0, r_0 = r_0,
psize = psize):
        self.type = 'Buffer'
        self.count = 1

```

```

self.speed = speed
self.ang_direction = direction
self.size = psize
self.angle = angle
self.rad = rad
self.r_0 = r_0
self.bound = []
self.attached = attached
if self.attached == maxBattached:
    self.status = 'Full'
elif self.attached < maxBattached:
    self.status='Free'
if self.attached == 0:
    self.color = 'black'
elif self.attached == 1:
    self.color = 'blue'
elif self.attached == maxBattached:
    self.color = 'red'
else:
    self.color = 'purple'
self.shape = component_loc(self.angle,self.rad,self.size,self.color)
self.x = pol2cart_x(self.angle,self.rad)
self.y = pol2cart_y(self.angle,self.rad)
self.coords = [self.x, self.y]
componentList.append(self)
def buffer_direction(self):
    counter = 0
    x = []
    for component in componentList:
        if ((component.type == 'Buffer') and (component != self)):
            distance = math.hypot(self.x-component.x,self.y-component.y)
            if distance <= 3*self.size:
                counter += 1
                x.append(component.coords)
    if counter == 0:
        return False
    return 'Collisions', x
def calcium_binding(self):
    counter = 0
    for component in componentList:
        if ((self.status == 'Free') and (component.type == 'Calcium') and (component.status ==
'Free')):
            distance = math.hypot(self.x-component.x,self.y-component.y)
            if distance < self.size:
                counter = 1
                self.bound.append([component,0])
                self.attached +=1
                component.status = 'B_bound'

```

```

        component.color = 'yellow'
        canvas.delete(component.shape)
        component.count = 0
        if self.attached == maxBattached:
            self.status = 'Full'
            self.color = 'red'
    if counter == 0:
        return False
    return self.status, self.bound, self.attached, self.color
def move(self):
    binding = self.calcium_binding()
    direction = self.buffer_direction()
    if direction == False:
        if self.rad < self.r_0 - self.size - self.speed:
            direct_x = random.randint(1,10)
            direct_y = random.randint(1,10)
            self.ang_direction = random.uniform(-pi,pi)
            self.x += (-1)**direct_x*self.speed*math.cos(self.ang_direction)
            self.y += (-1)**direct_y*self.speed*math.sin(self.ang_direction)
            self.rad = math.sqrt((self.x)**2+(self.y)**2)
            self.angle = math.atan2(self.y,self.x)
        else:
            self.ang_direction = random.uniform(self.angle-pi/6,self.angle+pi/6)
            self.x += -self.speed*math.cos(self.ang_direction)
            self.y += -self.speed*math.sin(self.ang_direction)
            self.rad = math.sqrt((self.x)**2+(self.y)**2)
            self.angle = math.atan2(self.y,self.x)
    elif direction[0] == 'Collisions':
        direct_x, direct_y = 0, 0
        if self.rad < self.r_0 - self.size - self.speed:
            for i in range(len(direction[1])):
                direct_x += self.x-direction[1][i][0]
                direct_y += self.y-direction[1][i][1]
            away = -math.atan2(direct_y,direct_x)
            self.x += self.speed*math.cos(away)
            self.y += self.speed*math.sin(away)
            self.rad = math.sqrt((self.x)**2+(self.y)**2)
            self.angle = math.atan2(self.y,self.x)
        else:
            self.ang_direction = random.uniform(self.angle-pi/6,self.angle+pi/6)
            self.x += -self.speed*math.cos(self.ang_direction)
            self.y += -self.speed*math.sin(self.ang_direction)
            self.rad = math.sqrt((self.x)**2+(self.y)**2)
            self.angle = math.atan2(self.y,self.x)
    if binding != False:
        self.color = binding[3]
        self.status = binding[0]
        self.bound = binding[1]

```

```

if binding[2] == 0:
    self.color = 'black'
elif binding[2] == 1:
    self.color = 'blue'
elif binding[2] == maxBattached:
    self.color = 'red'
else:
    self.color = 'purple'
for calcium in self.bound:
    if calcium[1] >= calcium_release:
        calcium[0].status = 'Free'
        calcium[0].color = 'green'
        calcium[0].count = 1
        i = self.bound.index(calcium)
        x = self.x + math.cos((-1)**i*pi/2)*self.size
        y = self.y + math.sin((-1)**i*pi/2)*self.size
        calcium[0].x = x
        calcium[0].y = y
        calcium[0].rad = math.hypot(x,y)
        calcium[0].angle = math.atan2(y,x)
        calcium[0].coords = [x,y]
        self.bound.remove(calcium)
self.attached = len(self.bound)
for i in range(self.attached):
    self.bound[i][1] += 1
if self.attached == maxBattached:
    self.status = 'Full'
elif self.attached < maxBattached:
    self.status='Free'
if self.attached == 0:
    self.color = 'black'
elif self.attached == 1:
    self.color = 'blue'
elif self.attached == maxBattached:
    self.color = 'red'
else:
    self.color = 'purple'
canvas.delete(self.shape)
self.shape = component_loc(self.angle,self.rad,self.size,self.color)
self.coords = [self.x,self.y]
self.ang_direction = direction
def destroy(self):
    canvas.delete(self.shape)
##### CALCIUM #####
class calcium():
    def __init__(self, Vattached = 0, status = 'Free', direction = 0, speed = calcium_speed, angle = 0,
rad = 0, r_0 = r_0, psize = psize):
    self.type = 'Calcium'

```

```

self.count = 1
self.Vattached = Vattached
self.status = status
self.speed = speed
self.ang_direction = direction
self.size = psize
self.angle = angle
self.rad = rad
self.r_0 = r_0
if self.Vattached == 1:
    self.status = 'V_Bound'
    self.color = 'pink'
    self.shape = component_loc(self.angle,self.rad,self.size,self.color)
elif self.status == 'Free':
    self.color = 'green'
    self.shape = component_loc(self.angle,self.rad,self.size,self.color)
elif self.status == 'B_bound':
    canvas.delete(self.shape)
self.x = pol2cart_x(self.angle,self.rad)
self.y = pol2cart_y(self.angle,self.rad)
self.coords = [self.x, self.y]
self.ang_coords = [self.rad,self.angle]
componentList.append(self)
def calcium_direction(self):
    counter = 0
    x = []
    for component in componentList:
        if ((component.type == 'Calcium') and (component != self)):
            distance = math.hypot((self.x+self.size/2)-
(component.x+component.size/2),(self.y+self.size/2)-(component.y+component.size/2))
            if distance <= 3*self.size:
                counter += 1
                x.append(component.coords)
    if counter == 0:
        return False
    return 'Collisions', x
def move(self):
    if self.status == 'Free':
        direction = self.calcium_direction()
        if direction == False:
            if self.rad < self.r_0 - self.size - self.speed:
                direct_x = random.randint(1,2)
                direct_y = random.randint(1,2)
                self.ang_direction = random.uniform(-pi,pi)
                self.x += (-1)**direct_x*self.speed*math.cos(self.ang_direction)
                self.y += (-1)**direct_y*self.speed*math.sin(self.ang_direction)
                self.rad = math.sqrt((self.x)**2+(self.y)**2)
                self.angle = math.atan2(self.y,self.x)

```

```

elif self.rad > self.r_0 + (width/2-self.r_0)/2:
    direct_x = random.randint(1,10)
    direct_y = random.randint(1,10)
    self.ang_direction = random.uniform(-pi,pi)
    self.x += (-1)**direct_x*self.speed*math.cos(self.ang_direction)
    self.y += (-1)**direct_y*self.speed*math.sin(self.ang_direction)
    self.rad = math.sqrt((self.x)**2+(self.y)**2)
    self.angle = math.atan2(self.y,self.x)
else:
    self.ang_direction = random.uniform(self.angle-pi/6,self.angle+pi/6)
    self.x += -self.speed*math.cos(self.ang_direction)
    self.y += -self.speed*math.sin(self.ang_direction)
    self.rad = np.sqrt((self.x)**2+(self.y)**2)
    self.angle = math.atan2(self.y,self.x)
elif direction[0] == 'Collisions':
    direct_x, direct_y = 0, 0
    if self.rad < self.r_0 - self.size - self.speed:
        for i in range(len(direction[1])):
            direct_x += self.x-direction[1][i][0]
            direct_y += self.y-direction[1][i][1]
        away = -math.atan2(direct_y,direct_x)+random.choice([-1,0,1])*pi/2
        self.x += self.speed*math.cos(away)
        self.y += self.speed*math.sin(away)
        self.rad = math.sqrt((self.x)**2+(self.y)**2)
        self.angle = math.atan2(self.y,self.x)
    elif self.rad > self.r_0 + (width/2-self.r_0)/2:
        direct_x, direct_y = 0, 0
        for i in range(len(direction[1])):
            direct_x += self.x-direction[1][i][0]
            direct_y += self.y-direction[1][i][1]
        away = -math.atan2(direct_y,direct_x)+random.choice([-1,0,1])*pi/2
        self.x += self.speed*math.cos(away)
        self.y += self.speed*math.sin(away)
        self.rad = math.sqrt((self.x)**2+(self.y)**2)
        self.angle = math.atan2(self.y,self.x)
    else:
        self.ang_direction = random.uniform(self.angle-pi/6,self.angle+pi/6)
        self.x += -self.speed*math.cos(self.ang_direction)
        self.y += -self.speed*math.sin(self.ang_direction)
        self.rad = np.sqrt((self.x)**2+(self.y)**2)
        self.angle = math.atan2(self.y,self.x)
elif self.status == 'V_bound':
    self.rad = math.hypot(self.x,self.y)
    self.angle = math.atan2(self.y,self.x)

canvas.delete(self.shape)
self.shape = component_loc(self.angle,self.rad,self.size,self.color)
self.coords = [self.x,self.y]

```

```

        direction = self.ang_direction
        if self.status == 'B_bound':
            canvas.delete(self.shape)
    def destroy(self):
        canvas.delete(self.shape)
##### INITIALIZE #####
def initialize():
    print('start')
    global componentList
    for component in componentList:
        if component.type in ['Buffer','Calcium']:
            canvas.delete(component.shape)
    bufferList, calciumList = [], []
    for i in range(buffer_initial):
        Buffer(angle = math.radians(random.randrange(10,360,10)), rad = random.randrange(10,r_0-
2*psize,3))
    for j in range(calcium_initial):
        calcium(angle = math.radians(random.randrange(10,360,10)), rad =
random.triangular(10,width/2-psize,width/2-20))
    canvas.update()
    for i in range(vesicle_initial):
        vesicle(sector = i)
    initialize()
def update_all():
    for component in componentList:
        component.move()
for i in range(runs):
    update_all()
    canvas.update()
canvas.mainloop()

```